

## Temperature histories in liquid and solid polar stratospheric cloud formation

Niels Larsen,<sup>1</sup> Bjørn M. Knudsen,<sup>1</sup> James M. Rosen,<sup>2</sup> Norman T. Kjome,<sup>2</sup> Roland Neuber,<sup>3</sup> and Esko Kyrö<sup>4</sup>

**Abstract.** Polar stratospheric clouds (PSCs) have been observed by balloonborne backscatter sondes from Alert, Thule, Heiss Island, Scoresbysund, Sodankylä, Søndre Strømfjord, and Ny Ålesund during winters 1989, 1990, 1995, and 1996 in 30 flights. The observations can be categorized into two main groups: type 1a and type 1b PSC particles. Type 1b PSCs show the characteristics expected from liquid ternary solution ( $\text{HNO}_3/\text{H}_2\text{SO}_4/\text{H}_2\text{O}$ ) particles, consistent with model simulations. Type 1a PSCs are observed at all temperatures below the condensation temperature  $T_{\text{NAT}}$  of nitric acid trihydrate (NAT), consistent with solid NAT composition. Air parcel trajectories have been calculated for all observations to provide synoptic temperature histories of the observed particles. A number of cases have been identified, where the particles have experienced temperatures close to or above the sulfuric acid tetrahydrate melting temperatures within 20 days prior to observation. This assures a knowledge of the physical phase (liquid) of the particles at this time, prior to observation. The subsequent synoptic temperature histories, between melting and the time of observation, show pronounced differences for type 1a and type 1b PSC particles, indicating the qualitative temperature conditions, necessary to generate solid type 1a PSCs. The temperature histories of type 1b particles show smoothly, in most cases monotonic, decreasing temperatures. The temperature can apparently decrease to the frost point without causing the particles to freeze. The type 1b PSC particles are mostly observed shortly after entering a cold region. The observed type 1a particles have spent several days at temperatures close to or below  $T_{\text{NAT}}$  prior to observation, often associated with several synoptic temperature oscillations around  $T_{\text{NAT}}$ , and the particles are observed in aged clouds. It appears that the PSC particles may freeze, if they experience synoptic temperatures below  $T_{\text{NAT}}$  with a duration of at least 1 day, possibly accompanied by several temperature oscillations. However, liquid particles that experience a smooth cooling, even to very low temperatures, or single smooth cooling/heating below  $T_{\text{NAT}}$  without synoptic temperature fluctuations do not seem to freeze.

### 1. Introduction

It has been recognized for many years that the occurrence of polar stratospheric clouds at very low temperatures during winter is the main factor for initializing large chemical ozone depletions inside the polar vortices under the present conditions, characterized by elevated abundances of chlorine and bromine species [World Meteorological Organization (WMO), 1994]. The polar stratospheric clouds (PSCs) prime the winter stratosphere for chemical ozone destruction in two ways. First, heterogeneous chemical reactions convert chlorine and bromine reservoir compounds into potentially ozone-

destroying radicals. Second, heterogeneous reactions, and the condensation of nitric acid to form the particles, effectively deplete the gas phase of nitrogen. Reactive nitrogen would otherwise reduce the ozone destruction in the lower stratosphere by converting the halogen radicals back into the reservoir forms [Solomon, 1988, 1990; WMO, 1991, 1994]. Irreversible denitrification and dehydration occur when the PSC particles transport condensed  $\text{HNO}_3$  and  $\text{H}_2\text{O}$  by sedimentation to lower altitudes. The heterogeneous chemical reaction rates depend strongly on temperature and on the composition and physical phase of the particles [Molina *et al.*, 1993; Ravishankara and Hanson, 1996], and for denitrification to become effective, relatively large solid PSC particles must form. Therefore, in order to understand and model the detailed influence of PSCs on polar ozone depletion, the nature of the particles and their formation process must be known.

In situ measurements in PSCs have shown that the cloud particles contain nitric acid and water [Fahey *et al.*, 1989; Kawa *et al.*, 1990], but the exact composition and physical phase of the particles at different atmospheric conditions remain unclear. Two different types (1a and 1b) of PSCs, existing above the ice frost point, have been identified

<sup>1</sup>Danish Meteorological Institute, Copenhagen, Denmark.

<sup>2</sup>Department of Physics and Astronomy, University of Wyoming, Laramie.

<sup>3</sup>Alfred Wegener Institute for Polar and Marine Research, Potsdam, Germany.

<sup>4</sup>Finnish Meteorological Institute, Sodankylä, Finland.

Copyright 1997 by the American Geophysical Union.

Paper number 97JD01666.  
0148-0227/97/97JD-01666\$09.00

from lidar measurements [Browell *et al.*, 1990] in addition to type 2 PSC water ice particles which form below the frost point. Type 1b PSCs are presumably liquid particles [Toon *et al.*, 1990], and laboratory measurements and model calculations suggest that these particles could be composed of supercooled ternary solutions (STS;  $\text{HNO}_3/\text{H}_2\text{SO}_4/\text{H}_2\text{O}$ ) [Zhang *et al.*, 1993a; Molina *et al.*, 1993; Tabazadeh *et al.*, 1994; Drdla *et al.*, 1994; Carslaw *et al.*, 1994]. Solid type 1a PSCs were assumed to form by cocondensation of nitric acid and water [Crutzen and Arnold, 1986; Toon *et al.*, 1986] and might be composed of nitric acid trihydrate (NAT) since this is the stable hydrate at stratospheric conditions [Hanson and Mauersberger, 1988].

If type 1b PSC particles are composed of supercooled ternary solutions, then they will form by direct uptake of nitric acid and water from the gas phase, without nucleation. The direct uptake will be a smooth function of temperature and will result in a steep increase in total condensed volume at about 4 K below  $T_{\text{NAT}}$ . If this uptake occurs slowly, all the particles will be in equilibrium with the gas phase, and so all the particles will have the same composition [Tabazadeh *et al.*, 1994; Carslaw *et al.*, 1994].

The formation of solid type 1a PSC is difficult to explain, both from theoretical microphysics, laboratory studies, and field experiments [Tolbert, 1994]. Previously, it was assumed that NAT would form by heterogeneous nucleation on frozen sulfate aerosol particles. This picture has been questioned, at least as the initial PSC formation process in early winter, and perhaps generally in the Arctic. This is because laboratory experiments on bulk or thin-film supercooled ternary mixtures have indicated that freezing only takes place below [Koop *et al.*, 1995], or close to, the ice frost point [Molina *et al.*, 1993; Beyer *et al.*, 1994; Iraci *et al.*, 1994; Song, 1994; Fox *et al.*, 1995]. Laboratory experiments on binary sulfate and ternary solution aerosols have also shown that freezing of these particles takes place below the ice frost point [Bertram *et al.*, 1996; Imre *et al.*, 1997; Carleton *et al.*, 1997; Clapp *et al.*, 1997; Anthony *et al.*, 1997]. Furthermore, laboratory measurements [Iraci *et al.*, 1995] and nucleation theory [MacKenzie *et al.*, 1995] have shown that NAT is unlikely to nucleate on frozen aerosol particles, composed of sulfuric acid tetrahydrate (SAT).

NAT nucleation might be possible on preactivated SAT surfaces. Zhang *et al.* [1996] found in laboratory experiments that SAT, which has once been involved in NAT formation, would be more suitable for NAT nucleation in a subsequent cooling. This mechanism may be important in later stages of PSC formation during winter in the Arctic. On the other hand, Koop and Carslaw [1996] argue from thermodynamical model calculations that SAT would melt during cooling below a deliquescence temperature ( $T_d$ ), roughly 2-3 K above the ice frost point, when  $\text{HNO}_3$  is present in the gas phase. According to this theory, SAT particles would transform into liquid supercooled ternary solutions by large  $\text{HNO}_3$  uptake, since SAT would be unstable in this temperature range with respect to STS.

Some predictions and perhaps mutual contradictions emerge from these two theories which observational studies should try to address. First, a prediction from the

Koop and Carslaw [1996] theory would be that deliquescence sets a well defined temperature limit, given by the ambient conditions, below which PSCs should form. This threshold lies between the temperature, where STS particles start their growth, and the deliquescence temperature, that is at roughly 4 K below  $T_{\text{NAT}}$ . Second, SAT particles in the stratosphere have presumably frozen below or close to the ice frost point. At that stage the particles are likely to have contained nitric acid in some form. Upon subsequent heating and evaporation of  $\text{HNO}_3$ , the remaining SAT core could be preactivated for NAT condensation. NAT may then condense on preactivated SAT in a subsequent cooling when saturation ratios of nitric acid over NAT reach about 10 [Zhang *et al.*, 1996]. This would seem to be in conflict with the constrain on deliquescence upon cooling, requiring this to occur before the nucleation of any  $\text{HNO}_3$  solid phase, and noting that SAT deliquescence would take place at lower temperatures around saturation ratios of 20-25 with respect to NAT [Koop and Carslaw, 1996].

As another aspect of solid particle formation, Meilinger *et al.* [1995] argued that very fast cooling in lee wave events would cause the composition of liquid particles to depart considerably from equilibrium. The small particles quickly adjust their composition toward equilibrium, while the large particles would not be able to maintain equilibrium due to slow diffusion in the gas phase, limiting their  $\text{HNO}_3$  uptake. The same nonequilibrium conditions could also prevail during SAT deliquescence without the requirement of fast cooling [Koop and Carslaw, 1996]. Thereby the smallest particles could approach the stoichiometric composition of NAT with very small amounts of  $\text{H}_2\text{SO}_4$  which, according to laboratory experiments, would favor the freezing. In this view, freezing into stable solid particles would start among the smallest particles in the size distribution [Meilinger *et al.*, 1995].

This study addresses the conditions for freezing to generate solid phase PSC particles. A large data set of PSC observations, obtained throughout a number of recent winter seasons by balloonborne backscatter sondes from various locations in the Arctic at low stratospheric temperatures, have been analyzed by means of isentropic airparcel trajectories, providing the synoptic temperature histories of the observed particles. The aim of the study is to identify cases where the particles, prior to observation, have been in the liquid phase, that is above or close to the SAT melting temperature [Middlebrook *et al.*, 1993; Zhang *et al.*, 1993b], and then, for these cases, to follow the remaining temperature history until the time of observation. The identified temperature history cases have then been grouped according to the observed properties of the particles (type 1a or 1b PSCs as defined below) and thereby form the basis for a qualitative analysis of freezing and the conditions where the particles stay in the liquid phase.

## 2. Measurements

The balloonborne backscatter sonde was developed by the University of Wyoming [Rosen and Kjöme, 1991] for measurements of stratospheric aerosol and cloud particles. An advantage of this instrument is that observations are made in

situ without affecting the particles. The instrument is equipped with a flash lamp, emitting strong horizontally directed beams approximately every 7 s during the balloon ascent and descent. The backscattered light from the particles, within a range of a few meters from the sonde, is measured by photodetectors with narrow band filters in two wavelengths around 940 and 480 nm. The ambient air pressure and temperature, together with ozone partial pressure, are measured with separate onboard sensors, simultaneously with the aerosol backscatter signal. The primary data products from the measurements are the aerosol backscatter ratios (particulate to molecular) at the two wavelengths (B<sub>940</sub> and B<sub>480</sub>). From this a color index *C* is simply defined as  $C = B_{940}/B_{480}$ .

In the following analysis, data are obtained in 30 flights from Alert (82.5°N, 62.3°W), Heiss Island (80.6°N, 58.1°E), Thule (Pituffik, 76.5°N, 68.8°W), Scoresbysund, (Illoqqortoormiut, 70.5°N, 22.0°W), Sodankylä (67.4°N, 26.6°E), Søndre Strømfjord (Kangerlussuaq, 67.0°N, 50.9°W), and Ny Ålesund (78.9°N, 11.9°E), performed in the winters 1989, 1990, 1995, and 1996. The measurements have been obtained at low stratospheric temperatures with the presence of PSCs on days when the stations were inside the polar vortex, as indicated by the potential vorticity on the 475 K potential temperature surface (cf. Table 1). During the three winters, following the volcanic eruption of Mount Pinatubo in June 1991, PSCs were not observed by backscatter sondes at the above stations. In Plate 1 are shown the vertical profiles of the aerosol backscatter ratio at 940 nm (black curves) and the color index (red curves) from all 30 flights. In this plot the vertical scale is the potential temperature between 350 K ( $\approx$  12 km) and 575 K ( $\approx$  23 km altitude), and the data in this plot have been smoothed, using a running mean with a 5 K window. The color index is only shown and used in the analysis at altitudes where the aerosol backscatter ratio is larger than 0.5 in order to have a good color index measurement. The blue and red hatched regions in the plots indicate the presence of type 1a and type 1b PSCs, respectively, as described in detail below. The 5 K-smoothed data are only used in connection with air parcel trajectories, which are calculated with a 5 K-vertical separation (cf. Figure 1 and Table 2 below), whereas the full data set is presented in comparisons with the measured temperatures in Plate 2.

In the following data analysis, the measured air temperatures are related to the condensation temperature of nitric acid trihydrate,  $T_{\text{NAT}}$  [Hanson and Mauersberger, 1988]. In order to calculate  $T_{\text{NAT}}$  a northern hemisphere limb infrared monitor of the stratosphere (LIMS) profile of nitric acid vapor mixing ratio [Gille and Russell, 1984] has been assumed together with a water vapor mixing ratio profile, increasing linearly from 4 to 6 parts per million by volume (ppmv) in the above potential temperature altitude range. Errors of 3 parts per billion by volume (ppbv) HNO<sub>3</sub> ( $\sim$ 30%) or 0.5 ppmv H<sub>2</sub>O ( $\sim$ 10%) would imply an error in  $T_{\text{NAT}}$  of about 0.5 K.

Plate 2a shows a scatterplot of the observed aerosol backscatter ratios at 940 nm against the color index from measurements in the above altitude range at temperatures between  $T_{\text{NAT}} + 8$  K and the ice frost point (at roughly 7 K below  $T_{\text{NAT}}$ ). Apparently, the particle observations fall into two main categories: one group of particles showing large variability in the aerosol backscatter ratio with color indices in a narrow range around 5-8 (red symbols), while another

**Table 1.** Flight Number, Location, and Date of the Backscatter Soundings, Together With the Potential Vorticity on the 475 K Surface (PV<sub>475</sub>) on the Day of the Flight at 12.00 UT

Flight	Location	Date	PV <sub>475</sub>
1	Alert	Jan. 9, 1989	57
2	Alert	Jan. 10, 1989	61
3	Alert	Jan. 13, 1989	54
4	Alert	Jan. 17, 1989	61
5	Alert	Jan. 21, 1989	64
6	Alert	Jan. 10, 1990	61
7	Alert	Jan. 13, 1990	54
8	Alert	Jan. 17, 1990	54
9	Alert	Jan. 20, 1990	54
10	Heiss Island	Jan. 26, 1989	55
11	Thule	Jan. 8, 1995	58
12	Thule	Jan. 10, 1995	51
13	Thule	Jan. 14, 1995	62
14	Scoresbysund	Jan. 3, 1995	52
15	Scoresbysund	Jan. 13, 1995	51
16	Sodankylä	Jan. 19, 1995	48
17	Thule	Jan. 11, 1996	47
18	Thule	Jan. 15, 1996	41
19	Thule	Jan. 16, 1996	47
20	Thule	Jan. 18, 1996	50
21	Thule	Jan. 21, 1996	60
22	Thule	Jan. 24, 1996	47
23	Scoresbysund	Feb. 16, 1996	52
24	Søndre Strømfjord	Jan. 8, 1996	40
25	Sodankylä	Feb. 14, 1996	51
26	Ny Ålesund	Jan. 6, 1996	47
27	Ny Ålesund	Jan. 14, 1996	43
28	Ny Ålesund	Jan. 17, 1996	38
29	Ny Ålesund	Jan. 21, 1996	49
30	Ny Ålesund	Feb. 12, 1996	48

PV<sub>475</sub> is in units of  $10^{-6} \text{ Km}^2\text{s}^{-1}\text{kg}^{-1}$ . Values larger than  $\approx$  40 PV units at this altitude indicate a location inside the edge of the polar vortex.

group of particles display relatively small aerosol backscatter ratios with large color indices (blue symbols). There also seem to be particles in a continuous transition range between the two main groups (black symbols). Somewhat similar groupings of lidar measurements of PSCs, based on depolarization, gave rise to the definitions of type 1b PSC (large scattering ratios and low depolarization) and type 1a PSC (low scattering and large depolarization) [Browell *et al.*, 1990], presumably reflecting the physical state of the particles (liquid and solid, respectively) [Toon *et al.*, 1990]. This categorization of the two distinct particle groups will be adopted here, assigning type 1a PSCs to particles with color index larger than 10, and type 1b PSCs to particles with color index between 5 and 8 or aerosol backscatter ratios larger than 15 as displayed in Plate 2a (blue and red symbols). It should be emphasized that the backscatter sonde does not directly measure the physical state of the particles, often associated with this categorization. However, the subsequent analysis will show that the grouping adopted here presumably also reflects the liquid and solid phase of the particles. In Plate 1

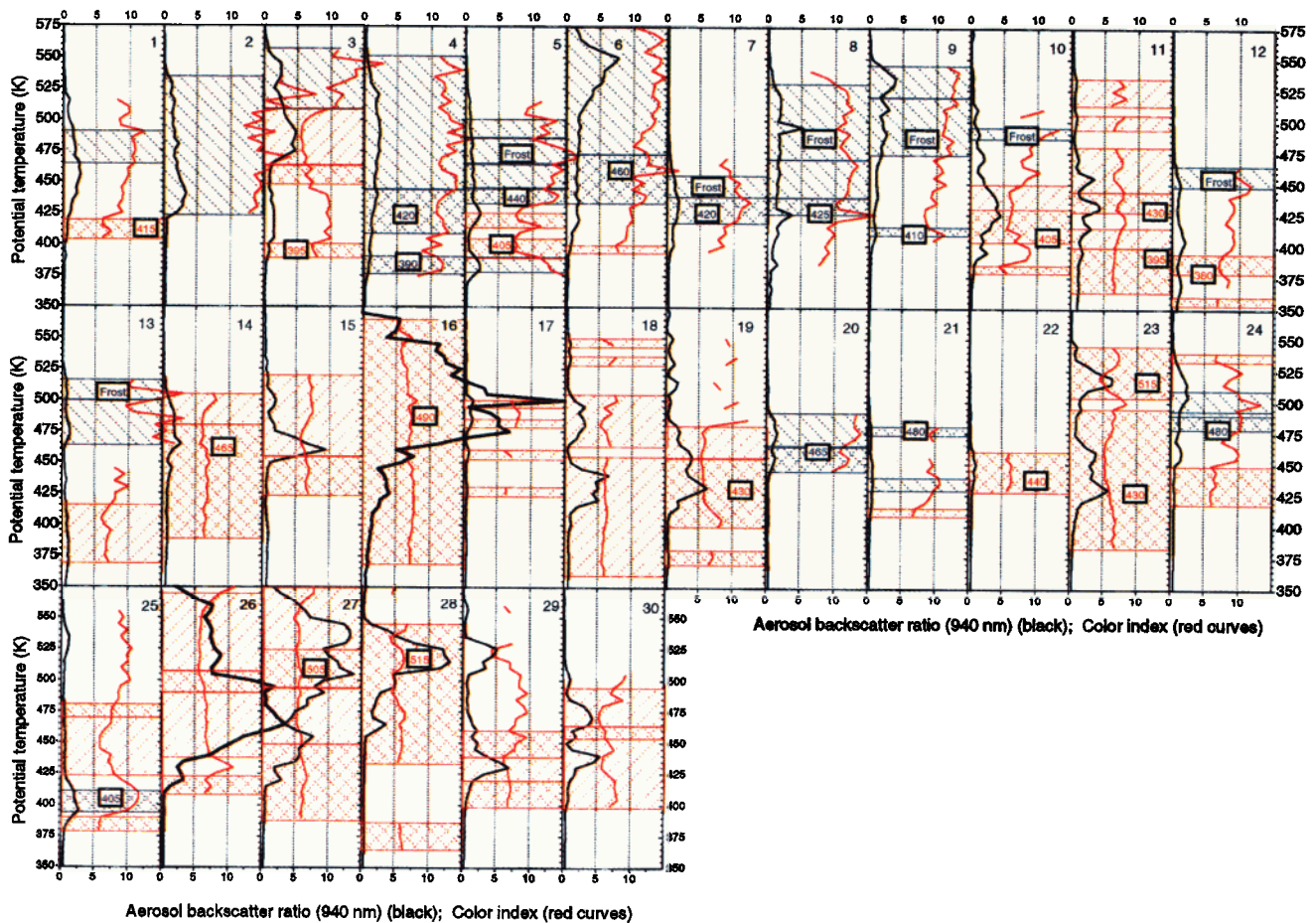


**Plate 1.** Vertical profiles of aerosol backscatter ratio at 940 nm (black curves) and color index (red curves) obtained in 30 flights (cf. Table 1). The altitude scale is potential temperature. The blue and red hatched altitude ranges correspond to the occurrence of type 1a and type 1b PSC particles according to the definition described in the text. Particles in the double-hatched altitude ranges have previously experienced SAT melting temperatures. The corresponding labels indicate the potential temperature altitude where the temperature history is presented in Plates 4 or 5, representative of the given altitude range. The label “Frost” indicates that the particles have previously experienced temperatures below the ice frost point for several days without subsequent melting.

the blue and red hatched altitude ranges indicate the presence of type 1a and type 1b PSCs, respectively, based on this definition.

With the same color coding as in Plate 2a, the measured aerosol backscatter ratios and color indices from all observations are plotted against the difference between the measured air temperature and the NAT condensation temperature in Plates 2b and 2c. From these plots it appears that type 1b PSCs (red symbols) at high temperatures possess low aerosol backscatter ratios which, at roughly 4 K below  $T_{\text{NAT}}$ , increase sharply (Plate 2b). On the other hand, type 1a PSCs (blue symbols) are observed predominantly at temperatures just below the NAT condensation temperature (Plate 2c). This is illustrated more clearly in Plate 2d where the observations have been grouped into 1 K temperature bins, showing the cumulative occurrence of type 1a (blue) and type 1b PSC observations (red curve) in the data set. Owing to the uncertainties in the assumed  $\text{HNO}_3$  and  $\text{H}_2\text{O}$  mixing ratios, the NAT condensation temperature cannot be calculated exactly, possibly explaining why a few type 1a particles are observed above the apparent  $T_{\text{NAT}}$  temperature.

Application of the Kolmogorov-Smirnov (KS) test [e.g., *Kendall and Stuart, 1979*] shows that the cumulative distribution function of type 1a observations in Plate 2d is significantly different from the distribution of type 1b observations (KS statistic equal to 0.29, corresponding to a significance level much less than 0.01% for the null hypothesis that the distributions are the same).

### 3. Data Analysis

Simulations have been performed to calculate the expected aerosol backscatter and color index from supercooled ternary solution particles. In these calculations a background binary ( $\text{H}_2\text{SO}_4/\text{H}_2\text{O}$ ) aerosol population has initially been assumed, described by a lognormal size distribution with 10 particles per  $\text{cm}^3$ , median radius of  $0.0725 \mu\text{m}$ , and geometric standard deviation of 1.86, corresponding to 0.9 parts per billion by mass (ppbm) of condensed  $\text{H}_2\text{SO}_4$ . The particles, at 50 hPa pressure altitude, have been cooled from 10 K above the ice frost point down to  $T_{\text{ice}}$ , assuming initially gas phase concentrations of 5 ppmv  $\text{H}_2\text{O}$  and 8.4 ppbv  $\text{HNO}_3$ , and

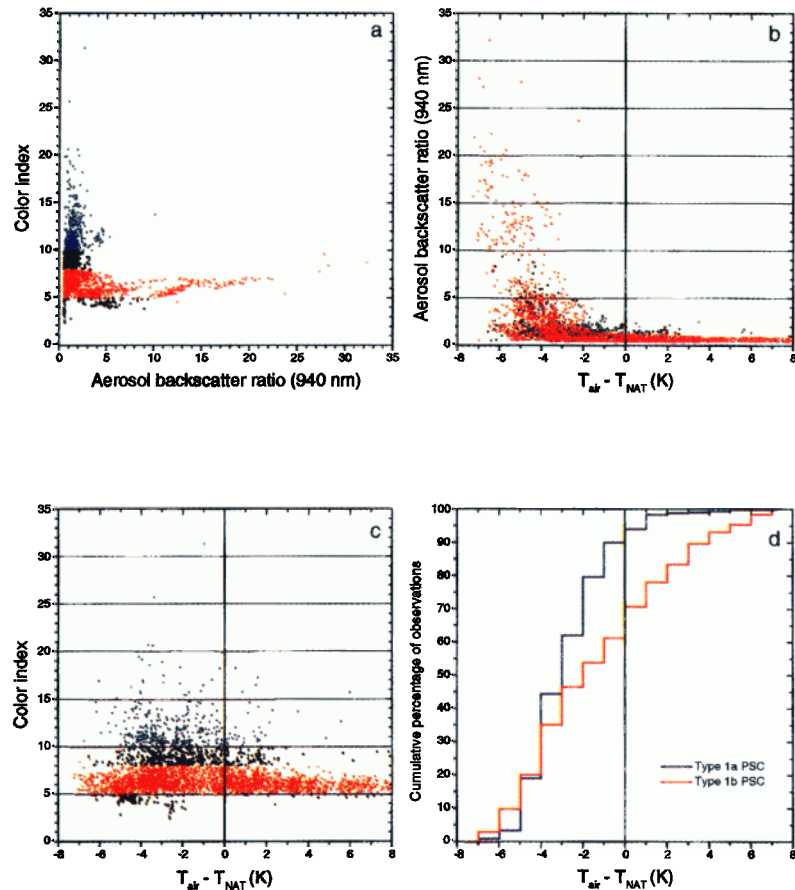


**Plate 2.** (a): Scatterplot of the observed color index plotted versus the aerosol backscatter ratio at 940 nm from all measurements where the particles have previously felt the SAT melting. Blue, red, and black symbols indicate type 1a PSC, type 1b PSC, and the transition particles, respectively. (b): Aerosol backscatter ratio and (c): color index of the same observations and color coding as in Plate 2a, plotted against the difference between the measured air temperature and the NAT condensation temperature. (d): The 397 type 1a and 2221 type 1b PSC observations, grouped into 1 K temperature bins, showing the cumulative occurrence of the observations.

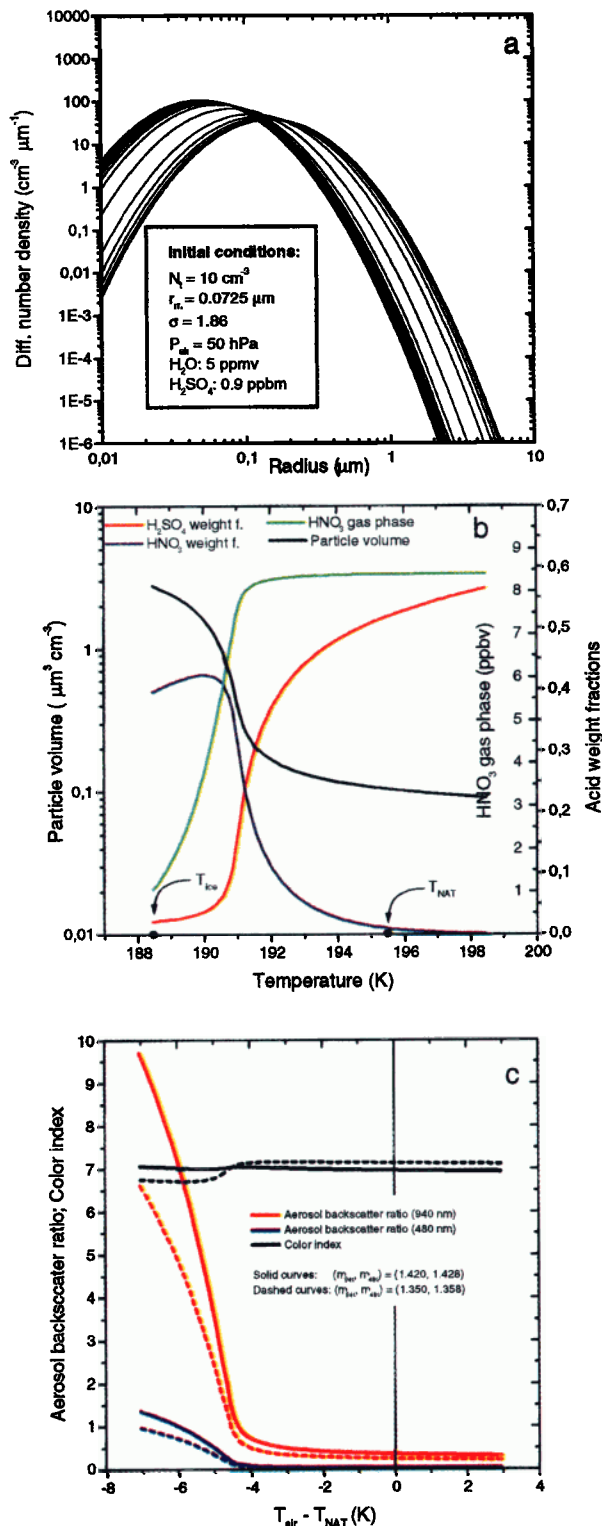
assuming the particles to reach equilibrium at each temperature step. To calculate the supercooled ternary solution compositions at low temperatures, the  $\text{HNO}_3$  and  $\text{H}_2\text{O}$  vapor pressure expressions given by Luo *et al.* [1995] have been used. Plate 3a shows the simulated growth in the aerosol size distribution every 0.5 K during the cooling, while the particles take up significant amounts of nitric acid and water from the gas phase and change the composition, as displayed in Plate 3b. The sharp increase in the particle volume takes place at roughly 4 K below  $T_{\text{NAT}}$  (black curve in Plate 3b), while the particle composition changes from sulfuric to nitric acid dominance (red and blue curves), and the gas phase is depleted of  $\text{HNO}_3$  (green curve).

Mie scattering theory [Bohren and Huffman, 1983] has been applied to calculate aerosol backscatter ratio at the two wavelengths, 940 and 480 nm, as it would be observed by the backscatter sonde [Larsen *et al.*, 1994]. Here two different sets of the real part of the refractive index,  $(m_{940}, m_{480}) = (1.420, 1.428)$  and  $(1.350, 1.358)$ , have been assumed, reflecting the possible decrease of refractive index at lower temperatures where the particles approach the  $\text{HNO}_3/\text{H}_2\text{O}$  composition [Luo *et al.*, 1996]. The results are displayed in Plate 3c with solid and dashed curves, representing the two

sets of refractive indices at high and low temperatures respectively. The calculations show the sharp increase in aerosol backscatter ratio (red and blue curves) at 4 K below  $T_{\text{NAT}}$  with nearly constant color index (black curves) at all temperatures. The results are in good agreement with the observed properties of type 1b PSC (red symbols in Plates 2b and 2c), supporting the assumption that these particles are composed of liquid supercooled ternary solutions. It should be noticed that the calculated aerosol backscatter ratios are proportional to the assumed initial particle number density which, however, does not influence the calculated nearly constant color ratios and the sharp increase in backscatter ratios at 4 K below  $T_{\text{NAT}}$ . Similarly, uncertainties in the assumed median radius and geometric standard deviation of the initial size distribution could explain the scatter in observed color ratios around the calculated values. Originally, the strongest evidence of the existence of STS particles in the stratosphere has come from a single ER-2 flight [Dye *et al.*, 1992; Drdla *et al.*, 1994; Carslaw *et al.*, 1994]. Other in situ airborne [Dye *et al.*, 1996], satellite [Massie *et al.*, 1997], and ground-based lidar measurements [Beyerle *et al.*, 1997] added confidence to the assumptions about STS particles. The present analysis, based on a large data set from different

winters, gives further experimental evidence that certain PSCs, classified as type 1b from their backscatter signatures, have scattering properties consistent with the assumption of the particles being composed of STS.

Measurements of large color indices have been associated with large solid particles [Rosen *et al.*, 1993]. As shown in Plates 2c and 2d, the observations of large color ratios are obtained predominantly close to or below the NAT



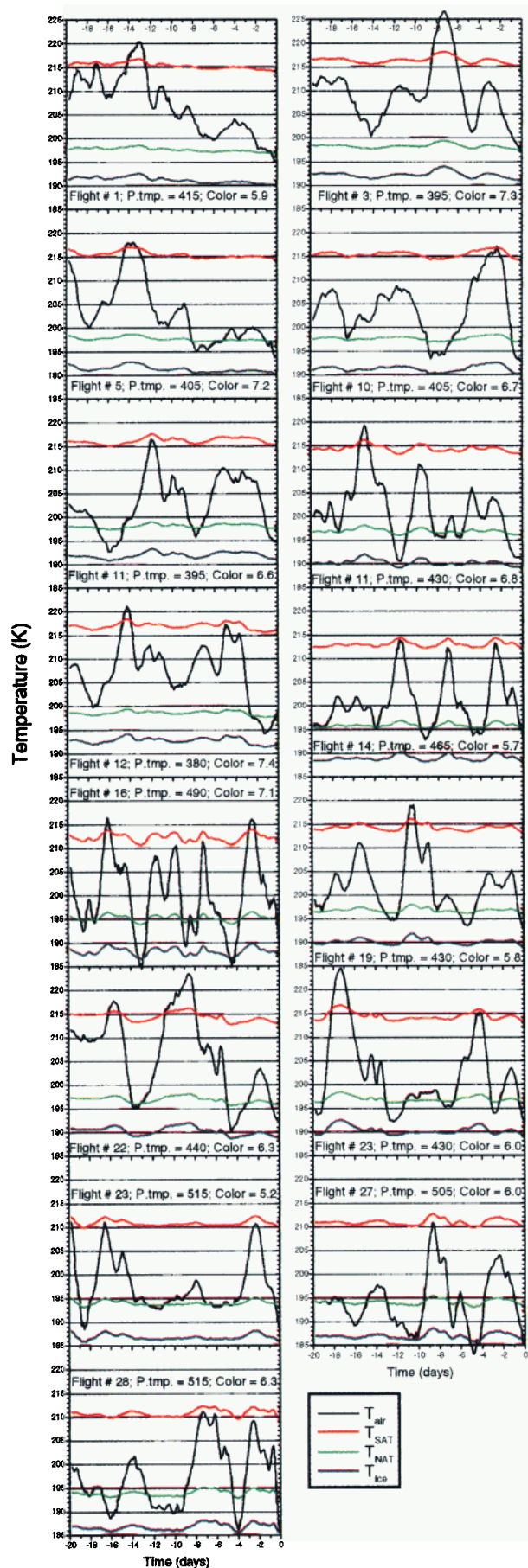
condensation temperature. Larsen *et al.* [1996] also showed that the particles retain their large color indices at temperatures lower than and up to  $T_{\text{NAT}}$  during evaporation. This indicates the composition of these particles to be crystalline nitric acid trihydrate, since a dilute metastable phase would evaporate at lower temperatures. Detailed inspection of the vertical profiles reveals that the color index in thick type 1b clouds (e.g., flights 16, 26, and 27, cf. Plate 1) only have a small scatter around the vertically running mean values, while this scatter is larger in type 1a clouds. The color index reflects the properties of the observed particles and does not directly depend on the ambient atmospheric conditions (pressure, temperature). Therefore the small scatter of color indices in type 1b PSCs possibly reflects the more homogeneous properties of liquid spherical particle in contrast to irregularly shaped solid type 1a particles. Finally, the following analysis of temperature histories will show that particles which possess the large color indices are in the solid state.

The particles with color indices between 8 and 10 (black symbols in Plate 2) could be solid, liquid, perhaps small solid metastable particles, or mixtures of different particle types which cannot be determined. However, in order to clearly discriminate between the two particle types (1a and 1b) the gap in color index between 8 and 10 has arbitrarily been adopted, although this designation does not necessarily reflect a specific property of the particles.

For each flight (Plate 1), 20-day backward isentropic air parcel trajectories, at every 5 K potential temperature between 350 and 575 K altitudes, have been calculated, based on the analyzed wind and temperature fields from the European Centre for Medium-Range Weather Forecasts (ECMWF). These calculations are our best estimates of the synoptic temperature histories of the observed particles. Small differences (less than 2 K) between the measured temperature and the trajectory endpoint temperature have been added to the calculated temperatures throughout the trajectory.

In particular, cases have been identified where the temperatures, prior to observation, have been above the melting temperature of sulfuric acid tetrahydrate [Middlebrook *et al.*, 1993; Zhang *et al.*, 1993b]. This assures, with substantial confidence, a knowledge of the physical phase (liquid) of the corresponding particles at this time, prior to observation. For those cases the subsequent temperature history, until the time of observation, will give qualitative information on the conditions for particle freezing. These cases constitute the basis for the following analysis. The identified altitude ranges where the particles have experienced

**Plate 3.** Simulation of supercooled ternary solution particles during cooling from 10 K above the ice frost point down to  $T_{\text{ice}}$ . (a): Differential size distributions during the particle growth, drawn every 0.5 K; (b): H<sub>2</sub>SO<sub>4</sub> (red) and HNO<sub>3</sub> (blue) weight fractions of the particle composition, total particle volume density (black), and gas phase concentration of HNO<sub>3</sub>, plotted against temperature; and (c): expected aerosol backscatter ratio at 940 nm (red) and 490 nm (blue) and color index (black curves) of the simulated particle growth as a function of the difference between air temperature and the NAT condensation temperature, as it would be observed by the backscatter sonde, and assuming two different sets of the refractive indices.



temperatures close to (within 3 K) or above the SAT melting temperatures are indicated by double-hatching in Plate 1. The numbers on the plot in each of these altitude ranges indicate potential temperatures where examples of representative detailed temperature histories will be presented below.

Most of the particles did not go through the high SAT melting temperatures within 20 days prior to observation, and therefore the physical phase, backward in time, cannot be determined from the temperature histories. However, in some of these cases the air temperatures went below the ice frost point for several days before the particles were observed at higher temperatures. Presumably, those particles would freeze into ice below the frost point (if not already frozen) and stay in the solid phase until observation. The altitude ranges of these particles have been indicated by the label “Frost” in Plate 1. These cases may not be very interesting for the purpose of this study since freezing is expected when temperatures go below the frost point for longer periods. It should be noticed, however, that in all these cases the color index,  $C$ , is above 10, supporting the assumption that the adopted definition here of type 1a PSCs ( $C > 10$ ) corresponds to solid particles.

It appears from Plate 1 that type 1b PSCs, which have experienced the high SAT melting temperatures prior to observation, were seen in flights 1, 3, 5, 10, 11, 12, 14, 15, 16, 19, 22, 23, 24, 25, 26, 27, 28, 29, and 30 in the red, double-hatched altitude ranges. Examples of representative temperature histories of these liquid particles are shown in Plate 4. Similarly, type 1a PSCs, which at some time prior to observation were in the liquid state above the SAT melting temperature, were observed in flights 4, 5, 6, 7, 8, 9, 20, 21, 24, and 25 in the blue, double-hatched altitude ranges. Examples of representative temperature histories of these particles, which presumably froze in the time interval between the SAT melting and the observation, are shown in Plate 5.

#### 4. Discussion

The representative synoptic temperature histories of the type 1b PSC (Plate 4) all show a nearly monotonic smooth cooling prior to observation. Apparently, the temperature at some point in the back trajectory can approach and go below the ice frost point without causing a freezing of the particles as seen most clearly in flights 16, 22, 27, and 28, which show the expected behavior of liquid particles. Neither does a smooth temperature transition below  $T_{\text{NAT}}$  seem to cause an increase in the color index as seen in flights 19, 22, and 23. The representative synoptic temperature histories of type 1a PSC qualitatively show a different behavior (Plate 5). In all cases the temperatures display fluctuations close to or below  $T_{\text{NAT}}$  with a duration of several days. In no case do the synoptic trajectory temperatures go below the ice frost point.

For each trajectory, where SAT melting took place before observation, the average synoptic heating rate ( $dT/dt$ ) in the

**Plate 4.** Representative 20-day backward synoptic temperature histories of type 1b PSC particles which have previously experienced temperatures close to, or above, the SAT melting temperature, calculated at the potential temperatures corresponding to the red labels in Plate 1.

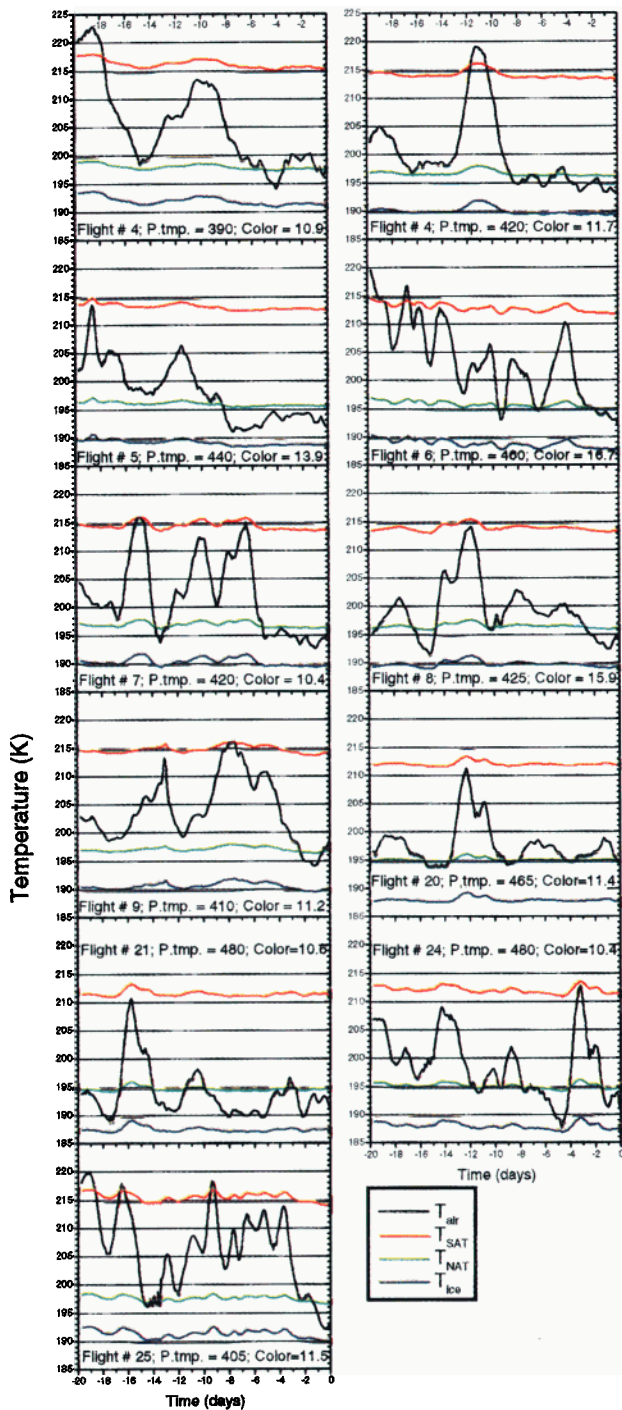


**Plate 5.** Same as Plate 4, but for type 1a PSC particles at the potential temperatures corresponding to the blue labels in Plate 1.

air parcel during the last 8 hours prior to observation has been calculated, together with the time spent at temperatures below  $T_{\text{NAT}}$  between melting and observation ( $\Delta t_{\text{NAT}}$ ). All trajectories in the double-hatched altitude ranges in Plate 1, and corresponding to observations obtained below  $T_{\text{NAT}}$ , have been considered here. The results have been grouped according to the observed PSC type, based on the mean value of color index (cf. Plate 1) in the 5 K window around the altitude of the trajectory. In Figure 1a is shown the histogram

of the number of observations (trajectories) at the different heating rates ( $dT/dt$ ) for type 1a and 1b PSCs. This plot clearly shows that the type 1b PSCs are predominantly observed at decreasing synoptic temperatures ( $dT/dt$  negative), whereas the type 1a PSCs are observed at both increasing and decreasing temperatures. Figure 1b similarly gives the histogram of  $\Delta t_{\text{NAT}}$ , showing that most of the type 1a PSCs have existed at temperatures below  $T_{\text{NAT}}$  for more than 1–2 days, while the type 1b PSC typically have spent less than 24 hours at low temperatures since melting, although in some cases (e.g., Plate 4, flight 11) this time could be rather long provided that temperature fluctuations do not occur in this period. Finally, Figure 1c shows for the two particle types how many times  $dT/dt$  has changed sign, shifting between synoptic cooling and heating or vice versa ( $n_{dT/dt}$ ), in the time interval between SAT melting and observation. Most type 1b PSCs experienced none or only a small number of synoptic temperature fluctuations, while type 1a PSCs generally felt more temperature fluctuations. Mean values and standard deviations of the mean of  $dT/dt$ ,  $\Delta t_{\text{NAT}}$ , and  $n_{dT/dt}$  are given in Table 2. Kolmogorov-Smirnov tests on the distributions in Figure 1 have been performed, and the KS statistics also appear in Table 2. The KS tests show that the type 1a and 1b PSC distributions, in each of the three panels in Figure 1, are significantly different (a significance level much less than 0.01% for the null hypothesis that the distributions in each of the panels are the same).

It should be noticed that errors in the trajectory temperatures and the estimated threshold temperatures of NAT and SAT make the analysis, as presented in Plates 4 and 5 and Figure 1, somewhat noisy, whereby strong quantitative statements about freezing are difficult to derive. The accuracy of the ECMWF analysis temperatures is generally better than 2 K [Knudsen, 1996], and no trajectories have been used in this study where the deviation between the measured and calculated endpoint temperature exceeds 2 K. It should be noticed, however, that the calculated temperature tendencies are more correctly estimated (i.e., increasing or decreasing temperatures in the last part of the trajectory, long or short duration at low temperatures since SAT melting, few or many shifts between synoptic heating and cooling since SAT melting, high temperatures in the vicinity of SAT melting), making the above findings on the qualitative features of the freezing conditions more certain.

Previously Larsen *et al.* [1996], based strictly on the temperature histories, grouped a subset of the present observational data according to a freezing scenario, suggested by Tabazadeh *et al.* [1995]. According to that theory, freezing might take place during heating after the particles have previously experienced a temperature close to the ice frost point. In the previous analysis a number (25%) of observations could not be classified since the assumed melting or freezing criteria were not fulfilled. However, for those particles which could be classified as liquid or solid, based solely on the temperature histories, the observed properties (aerosol backscatter ratio and color index) show the same features as seen in this analysis (Plate 2). Here the opposite approach has been taken where a subset of the particles, which are known to have been in the liquid state some time prior to observation, are classified based alone on the observed properties. The temperature histories of these type 1b (liquid) and type 1a (solid) particles are qualitatively consistent with the freezing criteria suggested by

Tabazadeh *et al.* [1995], although many quantitative uncertainties remain in this theory, concerning the low-temperature threshold and the number of cooling/heating cycles required to freeze all the particles. Lidar measurements of solid PSC particles from Sodankylä have also given some

support to the suggested freezing scenario [Wedekind *et al.*, 1996].

The synoptic scale temperature histories presented above may not be the actual temperatures experienced by the particles, since rapid mesoscale temperature fluctuations [Murphy and Gary, 1995] are not captured by the analyzed meteorological fields. Nevertheless, the systematic qualitative (Plates 4 and 5) and quantitative (Figure 1) differences between the synoptic temperature histories of type 1b and 1a PSCs are striking. It would be expected that an influence on particle freezing from random mesoscale temperature fluctuations during the history of the particles since SAT melting would tend to blur this categorization. The majority of the observations used in the present study were not obtained in typical lee wave areas (e.g., northern Scandinavia), and it is not obvious in the data set that mesoscale temperature fluctuations, to a large extent, have caused the freezing of the observed particles, compared to the more pronounced influence from the synoptic temperature histories. A similar conclusion was reached by Tabazadeh *et al.* [1996], who, based on a statistical approach of the influence of mesoscale temperature fluctuations on type 1a PSC formation, analyzed airborne lidar data, obtained over vast areas in the Arctic on January 11, 1989. It could also be noticed that the ER-2 in situ measurements of PSC particle size distributions from the same campaign on January 24 [Dye *et al.*, 1992], previously used to verify the equilibrium models of liquid ternary solution particles [Drdla *et al.*, 1994; Carslaw *et al.*, 1994], were obtained during a very long flight between northern Norway and Spitsbergen at nearly right angles to the wind at very low temperatures. All observed air parcels passed the Greenland ice cap (highest ground elevation in the Arctic) within 18-6 hours prior to the encounter with the aircraft [Poole *et al.*, 1990]. It is therefore likely that some of the particles had felt mesoscale temperature fluctuations, but still the STS properties of the observed particles are seen along a major part of the flight track without obvious signs of mesoscale temperature fluctuations causing the particles to freeze. Tabazadeh *et al.* [1995] presented a typical example of the temperature histories from the January 24 event, showing a strong monotonic synoptic cooling from temperatures above the SAT melting down to the observed low temperatures within 2

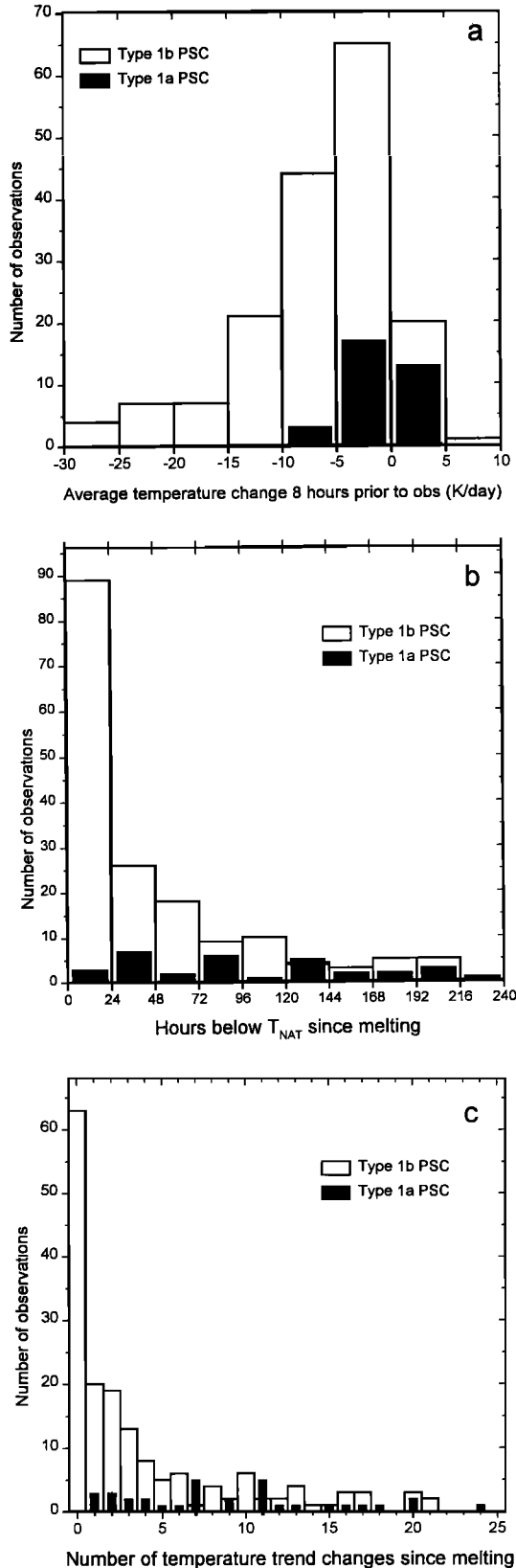


**Figure 1.** (a): Histogram of average synoptic heating rates ( $dT/dt$ ) during the last 8 hours before observation of particles which experienced the SAT melting prior to observation (double-hatched altitude ranges in Plate 1); (b): histogram of time spent below  $T_{NAT}$  between SAT melting and observation of the same particles; and (c): histogram of the number of times that the temperature history has changed from synoptic cooling ( $dT/dt < 0$ ) to heating ( $dT/dt > 0$ ) or vice versa of the same particles between SAT melting and observation. Each panel shows the histograms for type 1a and 1b PSC observations, categorized according to the average color index within the 5 K potential temperature window around the corresponding trajectory altitude. One hundred sixty-nine averaged observations (trajectories) are used for the type 1b, and 33 are used for the type 1a PSC distributions. Mean values of each distribution are given in Table 2. The data are binned in the same way for the two particle types, but the columns for type 1a PSC are shown slightly narrower to facilitate the comparison.

**Table 2.** Mean Values and Standard Deviations of Synoptic Heating Rates in Air Parcels ( $dT/dt$ ) During the Last 8 Hours Prior to Observation, the Time Spent Below  $T_{\text{NAT}}$  ( $\Delta t_{\text{NAT}}$ ) in the Time Interval Between SAT Melting and Observation, and the Number of Times That  $dT/dt$  Changed Sign in This Time Interval, Calculated for the Two Particle Types (cf. Figure 1)

	Type 1b PSC	Type 1a PSC	KS-Statistic	Figure 1 Panel
$dT/dt$ , K/day	$-6.0 \pm 0.5$	$-1.2 \pm 0.6$	0.51	a
$\Delta t_{\text{NAT}}$ , hours	$44 \pm 4$	$102 \pm 12$	0.58	b
$n_{dT/dt}$	$3.9 \pm 0.4$	$9.0 \pm 1.1$	0.51	c
No. of trajectories	169	33		

The table also gives the Kolmogorov-Smirnov (KS) statistics of the distributions in the three panels of Figure 1, and the number of trajectories used in the two particle categories.

days, consistent with the findings in the present study of the typical synoptic temperature histories of type 1b PSCs. Only two of our flights, 16 and 25 from Sodankylä, were performed downwind of high mountains where lee waves, large cooling rates, and temperature fluctuations below the ice frost point could be expected. In flight 16 (Plates 1 and 4) the synoptic temperatures dropped very fast below  $T_{\text{NAT}}$  just 10 hours before observation. In this flight, where temperatures close to the ice frost point were measured, clear signatures of liquid type 1b were observed throughout the vertical profile, except in a few very narrow layers with thickness of 20-30 meters where weak indications of solid particles were seen. In the other flight, number 25 (cf. Plates 1 and 5), the temperature stayed below  $T_{\text{NAT}}$  for 38 hours, and the type 1a particle properties were seen. Nonequilibrium effects could indeed play a decisive role for the PSC formation and characteristics in lee waves [Meilinger *et al.*, 1995]. However, for these two cases from potential lee wave regions, the observations are consistent with the general findings in the present study of the synoptic temperature history influence on the evolution of particle properties. In general, both types of PSC particles have probably experienced mesoscale temperature fluctuations of the same magnitude as the synoptic oscillations of type 1a PSC particles. This may indicate that the long duration at synoptic temperatures below  $T_{\text{NAT}}$  (Figure 1b) is a stronger requirement for freezing than the mere number of synoptic temperature oscillations below  $T_{\text{NAT}}$ , despite the differences in  $n_{dT/dt}$  for the two particle types as shown in Figure 1c.

In many of the solid particle temperature histories (cf. Plate 5), nitric acid could have evaporated and condensed repeatedly before observation, thereby occasionally releasing a frozen SAT core. According to Koop and Carslaw [1996], deliquescence sets a temperature limit ( $T_d$ ) below which the formation of type 1 PSCs must occur, independent of whether the initial particles are liquid or frozen as known  $\text{H}_2\text{SO}_4$  hydrates. Although this melting upon cooling theory may pertain only to the PSC formation phase, that is at decreasing temperatures, it does have some consequences for the further particle development after melting (deliquescence) when temperatures oscillate between  $T_{\text{NAT}}$  and  $T_{\text{ice}}$ . This could be illustrated by looking, for example, at the type 1a PSC temperature history of flight 21 in Plate 5. Assuming for the discussion that this is the true temperature history of the particles, melting could be expected during the cooling between day -3 and -2, and the subsequent temperature history would imply that the particles stay in the liquid phase until observation, in contradiction to what is actually

measured. On the other hand, if nitric acid evaporated during the heating, releasing a preactivated SAT core above  $T_{\text{NAT}}$  around day -3, then NAT would subsequently be able to condense [Zhang *et al.* 1996], leading to a solid particle in agreement with the observation. Other similar examples can be found in the type 1a PSC data set, and by looking at Plate 2c it appears that type 1a PSCs occur at all temperatures below  $T_{\text{NAT}}$ , not exclusively below  $T_d$ , both factors indicating a disagreement with the Koop and Carslaw theory. It should be noticed, however, that if we only look at those observations in Plate 2, where the temperatures have decreased monotonically from above  $T_{\text{NAT}}$  down to the observed temperature (and the above examples do not fall into this category), a rather clear signature of STS particles appears. This may give some evidence of the deliquescence upon cooling theory. Therefore it remains difficult to determine uniquely from these observations if deliquescence has influenced the PSC formation at temperatures between  $T_{\text{NAT}}$  and  $T_d$ , or if preactivation and NAT condensation would prevent deliquescence upon cooling, as indicated in the above example.

Laboratory deposition experiments, performed at stratospheric conditions with high ratios of  $\text{H}_2\text{O}$  to  $\text{HNO}_3$  in the gas phase [Marti and Mauersberger, 1993], have indicated that the nitric acid condensed material initially could form as a dilute solid, possessing a higher  $\text{HNO}_3$  vapor pressure than over NAT, and which slowly transforms into thermodynamically stable NAT. Other laboratory measurements have indicated that metastable solid phases initially form before stable NAT [Worsnop *et al.*, 1993; Fox *et al.*, 1995], while Marti and Mauersberger [1994] observed the formation of nitric acid pentahydrate. Ground-based lidar measurements from Antarctica have indicated that solid type 1 PSC particles form when temperatures have been below  $T_{\text{NAT}}$  for a long time or have reached the ice frost point [Adriani *et al.*, 1995]. Observational evidence from the Arctic has been presented for the initial formation of numerous small solid PSC particles in a water-rich metastable phase of relatively high nitric acid vapor pressures, compared to NAT [Tabazadeh and Toon, 1996]. These measurements indicated that type 1a NAT PSC particles could form after being exposed to temperatures below  $T_{\text{NAT}}$  for more than 1 day without necessarily going through rapid mesoscale temperature fluctuations below the ice frost point [Tabazadeh *et al.*, 1996]. It has also been shown that in the initial stages of PSC formation a supercooled ternary solution composition of particles provides a better fit to Microwave Limb Sounder measurements of gas phase  $\text{HNO}_3$  abundances over

Antarctica, but after several days at low temperatures, a nitric acid dihydrate (NAD) or NAT composition provides a better fit to the  $\text{HNO}_3$  measurements (M.L. Santee et al., UARS Microwave Limb Sounder  $\text{HNO}_3$  observations: Implications for Antarctic polar stratospheric clouds, submitted to *Journal of Geophysical Research*, 1997). The results from the present study are consistent with the above findings in terms of the aging of the particles at temperatures below  $T_{\text{NAT}}$  to induce the transformation into stable and presumably large type 1a PSC particles.

Denitrification in the Arctic is associated with cold winters. In this region the mechanism to generate denitrification, or equivalently to form large PSC particles, is closely related to the details of the freezing process. A relatively slow transfer of nitric acid from initially formed metastable particles of high nitric acid vapor pressures onto stable NAT particles, starting among the largest particles, has been speculated to be a mechanism to deposit the available nitric acid in the gas phase onto a few, and thereby large, particles which would obtain significant fall velocities [Rosen et al., 1989; Larsen, 1991; Worsnop et al., 1993; Marti and Mauersberger, 1993; Tabazadeh and Toon, 1996]. The above mentioned field observations of aged NAT particles seem to be in agreement with this hypothesis. It appears that this mechanism could explain how denitrification [Fahey et al., 1990] could occur in huge homogeneous PSC clouds of synoptic scale, for example, over the North Atlantic and the Arctic Ocean. In contrast to this situation, localized PSC occurrence in lee waves, where specific vertical temperature profiles or nonequilibrium conditions may cause the formation of inhomogeneous layers with large particles [Wofsy et al., 1990; Deshler et al., 1994; Peter et al., 1994; Meilinger et al., 1995], could also be responsible for the observed denitrification or vertical redistribution of nitric acid at these locations [Arnold et al., 1997]. On the basis of our sparse data set from lee-wave regions this hypothesis cannot be assessed here, and it remains to be seen which of the two processes could be the dominant contributor to the occasionally large scale denitrification in the Arctic.

## 5. Conclusion

In this study we have investigated the influence of synoptic temperature histories on the physical properties of PSC particles. It appears from the presented observations that liquid type 1b PSC particles can be cooled to very low temperatures, approaching the ice frost point, without causing them to freeze. In a subsequent monotonic heating, the particles will survive in the liquid state. Most of the liquid type 1b particles are observed in the process of an ongoing, relatively fast, and continuous cooling from temperatures clearly above the NAT condensation temperature. The particles are mostly seen at the edge of a cloud shortly after they enter the cold area. On the other hand, it appears that a relatively long period, with a duration of at least 1-2 days, at temperatures below  $T_{\text{NAT}}$ , and possibly also accompanied by slow, synoptic temperature fluctuations, provide the conditions which may lead to the production of solid type 1a PSCs. Solid PSC particles are therefore expected to be observed in aged clouds.

**Acknowledgments.** The use of ECMWF meteorological data in this study is gratefully acknowledged. Very useful comments from

the reviewers are much appreciated. This work has been supported by the Commission of the European Union, the Danish Space Board, and the Commission for Scientific Research in Greenland. J.M.R. and N.T.K. were supported by the U.S. National Science Foundation through the Office of Polar Programs.

## References

- Adriani, A., T. Deshler, G. Di Donfrancesco, and G.P. Gobbi, Polar stratospheric clouds and volcanic aerosol during spring 1992 over McMurdo Station, Antarctica: Lidar and particle counter comparisons, *J. Geophys. Res.*, *100*, 25877-25897, 1995.
- Anthony, S.E., T.B. Onasch, R.T. Tisdale, R.S. Disselkamp, and M.A. Tolbert, Laboratory studies of ternary  $\text{H}_2\text{SO}_4/\text{HNO}_3/\text{H}_2\text{O}$  particles: Implications for polar stratospheric cloud formation, *J. Geophys. Res.*, *102*, 10777-10784, 1997.
- Arnold, F., V. Bürger, K. Gollinger, M. Roncossek, J. Schneider, and S. Spreng, Observations of nitric acid perturbations in the winter Arctic stratosphere: Evidence for sedimentation?, *J. Atmos. Chem.*, in press, 1997.
- Bertram, A.K., D.D. Patterson, and J.J. Sloan, Mechanisms and temperatures for the freezing of sulfuric acid aerosols measured by FTIR extinction spectroscopy, *J. Phys. Chem.*, *100*, 2376-2383, 1996.
- Beyer, K.D., S.W. Seago, H.Y. Chang, and M.J. Molina, Composition and freezing of aqueous  $\text{H}_2\text{SO}_4/\text{HNO}_3$  solutions under polar stratospheric conditions, *Geophys. Res. Lett.*, *21*, 871-874, 1994.
- Beyerle, G., B. Luo, R. Neuber, T. Peter, and I.S. McDermid, Temperature dependence of ternary solution particle volumes as observed by lidar in the Arctic stratosphere during 1992/93, *J. Geophys. Res.*, *102*, 3603-3609, 1997.
- Bohren, C.F., and D.R. Huffman, *Absorption and Scattering of Light by Small Particles*, 530 pp., J. Wiley, New York, 1983.
- Browell, E.V., C.F. Butler, S. Ismail, P.A. Robinette, A.F. Carter, N.S. Higdon, O.B. Toon, M.R. Schoeberl, and A.F. Tuck, Airborne lidar observations in the wintertime Arctic stratosphere: Polar stratospheric clouds, *Geophys. Res. Lett.*, *17*, 385-388, 1990.
- Carleton, K.L., D.M. Sonnenfroh, and W.T. Rawlins, Freezing behavior of single sulfuric acid aerosols suspended in a quadrupole trap, *J. Geophys. Res.*, *102*, 6025-6033, 1997.
- Carlaw, K.S., B.P. Luo, S.L. Clegg, T. Peter, P. Brimblecombe, and P.J. Crutzen, Stratospheric aerosol growth and  $\text{HNO}_3$  gas phase depletion from coupled  $\text{HNO}_3$  and water uptake by liquid particles, *Geophys. Res. Lett.*, *21*, 2479-2482, 1994.
- Clapp, M.L., R.F. Niedziela, L.J. Richwine, T. Dransfield, R.E. Miller, and D.R. Worsnop, Infrared spectroscopy of sulfuric acid/water aerosols: Freezing characteristics, *J. Geophys. Res.*, *102*, 8899-8907, 1997.
- Crutzen, P.J., and F. Arnold, Nitric acid cloud formation in the cold Antarctic stratosphere: A major cause for the springtime 'ozone hole,' *Nature*, *324*, 651-655, 1986.
- Deshler, T., T. Peter, R. Müller and P.J. Crutzen, The lifetime of lee-wave-induced ice particles in the Arctic stratosphere; 1, Balloonborne observations, *Geophys. Res. Lett.*, *21*, 1327-1330, 1994.
- Drdla, K., A. Tabazadeh, R.P. Turco, M.Z. Jacobson, J.E. Dye, C. Twohy, and D. Baumgardner, Analysis of the physical state of one Arctic polar stratospheric cloud based on observations, *Geophys. Res. Lett.*, *21*, 2475-2478, 1994.
- Dye, J.E., D. Baumgardner, B.W. Gandrud, S.R. Kawa, K.K. Kelly, M. Loewenstein, G.V. Ferry, and B.L. Gary, Particle size distributions in Arctic polar stratospheric clouds, growth and freezing of

- sulfuric acid droplets, and implications for cloud formation, *J. Geophys. Res.*, *97*, 8015-8034, 1992.
- Dye, J.E., et al., In-situ observations of an Antarctic polar stratospheric cloud: Similarities with Arctic observations, *Geophys. Res. Lett.*, *23*, 1913-1916, 1996.
- Fahey, D.W., K.K. Kelly, G.V. Ferry, L.R. Poole, J.C. Wilson, D.M. Murphy, M. Loewenstein, and K.R. Chan, In situ measurements of total reactive nitrogen, total water, and aerosol in a polar stratospheric cloud in the Antarctic, *J. Geophys. Res.*, *94*, 11299-11315, 1989.
- Fahey, D.W., K.K. Kelly, S.R. Kawa, A.F. Tuck, M. Loewenstein, K.R. Chan, and L.E. Heidt, Observations of denitrification and dehydration in the winter polar stratospheres, *Nature*, *344*, 321-324, 1990.
- Fox, L.E., D.R. Worsnop, M.S. Zahniser, and S.C. Wofsy, Metastable phases in polar stratospheric clouds, *Science*, *267*, 351-355, 1995.
- Gille, J.C., and J.M. Russell III, The limb infrared monitor of the stratosphere: Experiment description, performance, and results, *J. Geophys. Res.*, *89*, 5125-5140, 1984.
- Hanson, D., and K. Mauersberger, Laboratory studies of the nitric acid trihydrate: Implications for the south polar stratosphere, *Geophys. Res. Lett.*, *15*, 855-858, 1988.
- Imre, D.G., J. Xu, and A.C. Tridico, Phase transformations in sulfuric acid aerosols: Implications for stratospheric ozone depletion, *Geophys. Res. Lett.*, *24*, 69-72, 1997.
- Iraci, L.T., A.M. Middlebrook, M.A. Wilson, and M.A. Tolbert, Growth of nitric acid hydrates on thin sulfuric acid films, *Geophys. Res. Lett.*, *21*, 867-870, 1994.
- Iraci, L.T., A.M. Middlebrook, and M.A. Tolbert, Laboratory studies of the formation of polar stratospheric clouds: Nitric acid condensation on thin sulfuric acid films, *J. Geophys. Res.*, *100*, 20969-20977, 1995.
- Kawa, S.R., D.W. Fahey, L.C. Anderson, M. Loewenstein, and K.R. Chan, Measurements of total reactive nitrogen during the Airborne Arctic Stratospheric Expedition, *Geophys. Res. Lett.*, *17*, 485-488, 1990.
- Kendall, M., and A. Stuart, *The Advanced Theory of Statistics*, vol. 2, Charles Griffin, London, 1979.
- Knudsen, B.M., Accuracy of arctic stratospheric temperature analyses and the implications for the prediction of polar stratospheric clouds, *Geophys. Res. Lett.*, *23*, 3747-3750, 1996.
- Koop, T., and K.S. Carslaw, Melting of  $\text{H}_2\text{SO}_4 \cdot 4\text{H}_2\text{O}$  particles upon cooling: Implications for polar stratospheric clouds, *Science*, *272*, 1638-1641, 1996.
- Koop, T., U.M. Biermann, W. Raber, B.P. Luo, P.J. Crutzen, T. Peter, Do stratospheric aerosol droplets freeze above the ice frost point?, *Geophys. Res. Lett.*, *22*, 917-920, 1995.
- Larsen, N., Polar stratospheric clouds: A microphysical simulation model, *Sci. Rep.* 91-2, Dan. Meteorol. Inst., Copenhagen, 1991.
- Larsen, N., B. Knudsen, T.S. Jørgensen, A. di Sarra, D. Fuà, P. Di Girolamo, G. Fiocco, M. Cacciani, J.M. Rosen, and N. Kjome: Backscatter measurements of stratospheric aerosols at Thule during January-February 1992, *Geophys. Res. Lett.*, *21*, 1303-1306, 1994.
- Larsen, N., B.M. Knudsen, J.M. Rosen, N.T. Kjome, and E. Kyrö, Balloonborne backscatter observations of type 1 PSC formation: Inference about physical state from trajectory analysis, *Geophys. Res. Lett.*, *23*, 1091-1094, 1996.
- Luo, B., K.S. Carslaw, T. Peter, and S.L. Clegg, Vapour pressures of  $\text{H}_2\text{SO}_4/\text{HNO}_3/\text{HCl}/\text{HBr}/\text{H}_2\text{O}$  solutions to low stratospheric temperatures, *Geophys. Res. Lett.*, *22*, 247-250, 1995.
- Luo, B., U.K. Krieger, and T. Peter, Densities and refractive indices of  $\text{H}_2\text{SO}_4/\text{HNO}_3/\text{H}_2\text{O}$  solutions to stratospheric temperatures, *Geophys. Res. Lett.*, *23*, 3707-3710, 1996.
- MacKenzie, A.R., M. Kulmala, A. Laaksonen, and T. Vesala, On the theories of type 1 polar stratospheric cloud formation, *J. Geophys. Res.*, *100*, 11275-11288, 1995.
- Marti, J. and K. Mauersberger, Laboratory simulations of PSC particle formation, *Geophys. Res. Lett.*, *20*, 359-362, 1993.
- Marti, J. and K. Mauersberger, Evidence for nitric acid pentahydrate formed under stratospheric conditions, *J. Phys. Chem.*, *98*, 6897-6899, 1994.
- Massie, S.T., et al., Simultaneous observations of polar stratospheric clouds and  $\text{HNO}_3$  over Scandinavia in January 1992, *Geophys. Res. Lett.*, *24*, 595-598, 1997.
- Meilinger, S., T. Koop, B.P. Luo, T. Huthwelker, K.S. Carslaw, U. Krieger, P.J. Crutzen, and T. Peter, Size-dependent stratospheric droplet composition in mesoscale temperature fluctuations and their potential role in PSC freezing, *Geophys. Res. Lett.*, *22*, 3031-3034, 1995.
- Middlebrook, A.M., L.T. Iraci, L.S. McNeill, B.G. Koehler, M.A. Wilson, O.W. Saastad, M.A. Tolbert, and D.R. Hanson, Fourier transform-infrared studies of thin  $\text{H}_2\text{SO}_4/\text{H}_2\text{O}$  films: Formation, water uptake, and solid-liquid phase changes, *J. Geophys. Res.*, *98*, 20473-20481, 1993.
- Molina, M.J., R. Zhang, P.J. Woolbridge, J.R. McMahon, J.E. Kim, H.Y. Chang, and K.D. Beyer, Physical chemistry of the  $\text{H}_2\text{SO}_4/\text{HNO}_3/\text{H}_2\text{O}$  system: Implications for polar stratospheric clouds, *Science*, *251*, 1418-1423, 1993.
- Murphy, D.M., and B.L. Gary, Mesoscale temperature fluctuations and polar stratospheric clouds, *J. Atmos. Sci.*, *52*, 1753-1760, 1995.
- Peter, T., R. Müller, P.J. Crutzen, and T. Deshler, The lifetime of leewave-induced ice particles in the Arctic stratosphere, 2, Stabilization due to NAT-coating, *Geophys. Res. Lett.*, *21*, 1331-1334, 1994.
- Poole, L.R., S. Solomon, B.W. Gandrud, K.A. Powell, J.E. Dye, R.L. Jones, and D.S. McKenna, The polar stratospheric cloud event of January 24, 1989, 1, Microphysics, *Geophys. Res. Lett.*, *17*, 537-540, 1990.
- Ravishankara, A.R., and D.R. Hanson, Differences in the reactivity of type 1 polar stratospheric clouds depending on their phase, *J. Geophys. Res.*, *101*, 3885-3890, 1996.
- Rosen, J.M., and N.T. Kjome, Backscattersonde: A new instrument for atmospheric aerosol research, *Appl. Opt.*, *30*, 1552-1561, 1991.
- Rosen, J.M., S.J. Oltmans, and W.E. Evans, Balloon borne observations of PSCs, frost point, ozone, and nitric acid in the north polar vortex, *Geophys. Res. Lett.*, *16*, 791-794, 1989.
- Rosen, J.M., N.T. Kjome, and S.J. Oltmans, Simultaneous ozone and polar stratospheric cloud observations at South Pole Station during winter and spring 1991, *J. Geophys. Res.*, *98*, 12741-12751, 1993.
- Solomon, S., The mystery of the Antarctic ozone "hole," *Rev. Geophys.*, *26*, 131-148, 1988.
- Solomon, S., Progress towards a quantitative understanding of Antarctic ozone depletion, *Nature*, *347*, 347-354, 1990.
- Song, N., Freezing temperatures of  $\text{H}_2\text{SO}_4/\text{HNO}_3/\text{H}_2\text{O}$  mixtures: Implications for polar stratospheric clouds, *Geophys. Res. Lett.*, *21*, 2709-2712, 1994.
- Tabazadeh, A., and O.B. Toon, The presence of metastable  $\text{HNO}_3/\text{H}_2\text{O}$  solid phases in the stratosphere inferred from ER2 data, *J. Geophys. Res.*, *101*, 9071-9078, 1996.
- Tabazadeh, A., R.P. Turco, K. Drdla, and M.Z. Jacobson, A study of type 1 polar stratospheric cloud formation, *Geophys. Res. Lett.*, *21*, 1619-1622, 1994.

- Tabazadeh, A., O.B. Toon, and P. Hamill, Freezing behavior of stratospheric sulfate aerosols inferred from trajectory studies, *Geophys. Res. Lett.*, *22*, 1725-1728, 1995.
- Tabazadeh, A., O.B. Toon, B.L. Gary, J.T. Bacmeister, and M.R. Schoeberl, Observational constraints on the formation of Type 1a polar stratospheric clouds, *Geophys. Res. Lett.*, *23*, 2109-2112, 1996.
- Tolbert, M.A., Sulfate aerosols and polar stratospheric cloud formation, *Science*, *264*, 527-528, 1994.
- Toon, O.B., P. Hamill, R.P. Turco, and J. Pinto, Condensation of HNO<sub>3</sub> and HCl in the Winter Polar Stratosphere, *Geophys. Res. Lett.*, *13*, 1284-1287, 1986.
- Toon, O.B., E.V. Browell, S. Kinne, and J. Jordan, An analysis of lidar observations of polar stratospheric clouds, *Geophys. Res. Lett.*, *17*, 393-396, 1990.
- Wedekind, C. F., et al., Lidar observations of liquid and solid PSC at Sodankylä, in *Polar stratospheric ozone 1995*, edited by J.A. Pyle, N.R.P. Harris, and G.T. Amanatidis, Air Pollut. Res. Rep. 56, pp. 136-140, Eur. Comm., Brussels, 1996.
- Wofsy, S. C., R. J. Salawitch, J. H. Yatteau, M. B. McElroy, B. W. Gandrud, J. E. Dye, and D. Baumgardner, Condensation of HNO<sub>3</sub> on falling ice particles: Mechanism for denitrification of the polar stratosphere, *Geophys. Res. Lett.*, *17*, 449-452, 1990.
- World Meteorological Organization (WMO), Scientific assessment of ozone depletion: 1991, *Rep. 25*, Global Ozone Res. and Monit. Proj., Geneva, 1991.
- World Meteorological Organization (WMO), Scientific assessment of ozone depletion: 1994, *Rep. 37*, Global Ozone Res. and Monit. Proj., Geneva, 1994.
- Worsnop, D.R., L.E. Fox, M.S. Zahniser, and S.C. Wofsy, Vapor pressures of solid hydrates of nitric acid: Implications for polar stratospheric clouds, *Science*, *259*, 71-74, 1993.
- Zhang, R., P.J. Wooldridge, and M.J. Molina, Vapor pressure measurements for the H<sub>2</sub>SO<sub>4</sub>/HNO<sub>3</sub>/H<sub>2</sub>O and H<sub>2</sub>SO<sub>4</sub>/HCl/H<sub>2</sub>O systems: Incorporation of stratospheric acids into background sulfate aerosols, *J. Phys. Chem.*, *97*, 8541-8548, 1993a.
- Zhang, R., P.J. Wooldridge, J.P.D. Abbatt, and M.J. Molina, Physical chemistry of the H<sub>2</sub>SO<sub>4</sub>/H<sub>2</sub>O binary system at low temperatures: Stratospheric implications, *J. Phys. Chem.*, *97*, 7351-7358, 1993b.
- Zhang, R., M.-T. Leu, and M.J. Molina, Formation of polar stratospheric clouds on preactivated background aerosols, *Geophys. Res. Lett.*, *23*, 1669-1672, 1996.
- 
- N. T. Kjome and J. M. Rosen, Department of Physics and Astronomy, University of Wyoming, Laramie, WY 82071. (e-mail: kjome@uwyo.edu; wyojim@igc.apc.org)
- B. M. Knudsen, and N. Larsen, Danish Meteorological Institute, Lyngbyvej 100, DK-2100 Copenhagen, Denmark. (e-mail: bk@dmi.dk; nl@dmi.dk)
- E. Kyrö, Finnish Meteorological Institute, Sodankylä Observatory, SF-99600 Sodankylä, Finland. (e-mail: esko.kyro@fmi.fi)
- R. Neuber, Alfred Wegener Institute for Polar and Marine Research, Telegrafenberg A43, D-14473 Potsdam, Germany. (e-mail: neuber@awi-potsdam.de)

(Received December 23, 1996; revised May 30, 1997; accepted June 5, 1997.)